

Theoretical direct WIMP detection rates for transitions to excited states.

J.D. Vergados¹, H. Ejiri² and K. G. Savvidy³

¹ *Theoretical Physics, University of Ioannina, Ioannina, Gr 451 10, Greece*

² *RCNP, Osaka University, Osaka, 567-0047, Japan and*

Nuclear Science, Czech Technical University, Brehova, Prague, Czech Republic. and

³ *Department of Physics, Nanjing University, Hankou Lu 22, Nanjing, 210098, China*

(Dated: March 6, 2018)

The recent WMAP and Planck data have confirmed that exotic dark matter together with the vacuum energy (cosmological constant) dominate in the flat Universe. Many extensions of the standard model provide dark matter candidates, in particular Weakly Interacting Massive Particles (WIMPs). Thus the direct dark matter detection is central to particle physics and cosmology. Most of the research on this issue has hitherto focused on the detection of the recoiling nucleus. In this paper we study transitions to the excited states, possible in some nuclei, which have sufficiently low lying excited states. Good examples are the first excited states of ¹²⁷I and ¹²⁹Xe. We find appreciable branching ratios for the inelastic scattering mediated by the spin cross sections. So, in principle, the extra signature of the gamma ray following the de-excitation of these states can, in principle, be exploited experimentally.

PACS numbers: 95.35.+d, 12.60.Jv 11.30Pb 21.60-n 21.60 Cs 21.60 Ev

I. INTRODUCTION

The combined MAXIMA-1 [1], BOOMERANG [2], DASI [3] and COBE/DMR Cosmic Microwave Background (CMB) observations [4] imply that the Universe is flat [5] and that most of the matter in the Universe is Dark [6], i.e. exotic. These results have been confirmed and improved by the recent WMAP [7] and Planck [8] data. Combining the data of these quite precise measurements one finds:

$$\Omega_b = 0.0456 \pm 0.0015, \quad \Omega_{\text{CDM}} = 0.228 \pm 0.013, \quad \Omega_\Lambda = 0.726 \pm 0.015$$

(the more recent Planck data yield a slightly different combination $\Omega_{\text{CDM}} = 0.274 \pm 0.020$, $\Omega_\Lambda = 0.686 \pm 0.020$). It is worth mentioning that both the WMAP and the Planck observations yield essentially the same value of $\Omega_m h^2$, but they differ in the value of h , namely $h = 0.704 \pm 0.013$ (WMAP) and $h = 0.673 \pm 0.012$ (Planck). Since any “invisible” non exotic component cannot possibly exceed 40% of the above Ω_{CDM} [9], exotic (non baryonic) matter is required and there is room for cold dark matter candidates or WIMPs (Weakly Interacting Massive Particles).

Even though there exists firm indirect evidence for a halo of dark matter in galaxies from the observed rotational curves, see e.g. the review [10], it is essential to directly detect such matter in order to unravel the nature of the constituents of dark matter. At present there exist many such candidates: the LSP (Lightest Supersymmetric Particle) [11–17], technibaryon [18, 19], mirror matter [20, 21], Kaluza-Klein models with universal extra dimensions [22, 23] etc. Additional theoretical tools are the structure of the nucleus see e.g. [24–27], and the nuclear matrix elements [28–32].

In most calculations the WIMP is supposed to be the neutralino or LSP (lightest supersymmetric particle), which is assumed to be primarily a gaugino, usually a bino. Models which predict a substantial fraction of higgsino lead to a relatively large spin induced cross section due to the Z-exchange. Such models tend to violate the LSP relic abundance constraint and are not favored. Some claims have recently been made, however, to the effect that the WMAP relic abundance constraint can be satisfied in the hyperbolic branch of the allowed SUSY parameter space, even though the neutralino is then primarily a higgsino [33]. We will not restrict ourselves in supersymmetry and we will adopt the optimistic view that the detection rates due to the spin may be large enough to be exploited by the experiments, see, e.g., [33] [34], [35], [30]. Such a view is further encouraged by the fact that, unlike the scalar interaction, the axial current allows one to populate excited nuclear states, provided that their energies are sufficiently low so that they are accessible by the low energy LSP, a prospect proposed long time ago [36] and considered in some detail by Ejiri and collaborators [37]. For a Maxwell-Boltzmann (M-B) velocity distribution the average kinetic energy of the WIMP

is:

$$\langle T \rangle \approx 50 \text{ keV} \frac{m_\chi}{100 \text{ GeV}} \quad (1)$$

So for sufficiently heavy WIMPs the average energy may exceed the excitation energy, e.g. of 57.7 keV for the $7/2^+$ excited state of ^{127}I and 39.6 keV for the first excited $3/2^+$ of ^{129}Xe . These are nuclei employed as targets in the ongoing dark matter searches. In other words one can explore the high velocity window, up to the escape velocity of $v_{esc} \approx 550 - 620 \text{ km/s}$. From a Nuclear Physics point of view this transition is not expected to be suppressed, since they appear to be allowed Gamow-Teller like.

II. THE STRUCTURE OF THE NUCLEI I-127 AND XE-129

As it has already been mentioned these nuclei are popular targets for dark matter detection. As a result the structure of their ground states has been studied theoretically by a lot of groups.

- The ^{127}I nucleus.

This is the most studied case. In this case we mention again the work of Ressel and Dean [28], the work of Engel, Pittel and Vogel [38], Vogel and Engel [39], Iachello, Krauss and Maiano [40], Nikolaev and Klapdor-Kleingrothaus [41] and later by Suhonen and collaborators [42]. In all these calculations for ^{127}I it appears that the spin matrix element is dominated by its proton component, which in our notation implies that the isoscalar and the isovector components are the same. In these calculations there appears to be a spread in the spin matrix elements ranging from 0.07 up to 0.354, in the notation of Ressel and Dean [28]. This, of course, implies discrepancies of about a factor of 25 in the event rates. Furthermore in the context of deformed nuclei [43] for the elastic case one finds:

$$\Omega_0^2 = \Omega_1^2 = \Omega_0 \Omega_1 = 0.164, \quad (2)$$

which is also smaller than the recent result [42], while for the transition to the excited state this model yields:

$$\Omega_0^2 = \Omega_1^2 = \Omega_0 \Omega_1 = 0.312 \quad (3)$$

In yet another calculation [44] in the case of the $A=127$ system it is reported that :

$$\Omega_0 = 1.001, \Omega_1 = 0.868 \text{ (elastic)}, \quad \Omega_0 = 0.098, \Omega_1 = 0.066 \text{ (inelastic)}$$

- Realistic calculations in the case of the Xe isotopes.

Such calculations relevant for elastic scattering have recently appeared [45]. For both elastic and inelastic scattering the above mentioned results [44] yield for ^{129}Xe :

$$\Omega_0 = 0.941, \Omega_1 = -0.954 \text{ (elastic)}, \quad \Omega_0 = 0.306, \Omega_1 = -0.311 \text{ (inelastic)}$$

Their spin structure functions are presented in Fig. 1.

In the present calculation we are going to employ the last two sets of spin nuclear matrix elements (a summary of some nuclear ME involved in elastic scattering can be found elsewhere [46]).

III. THE FORMALISM FOR THE WIMP-NUCLEUS DIFFERENTIAL EVENT RATE

The expression for the elastic differential event rate is well known, see e.g. [46]. The time averaged rate can be cast in the form:

$$\left. \frac{dR_0}{dE_R} \right|_A = \frac{\rho_\chi}{m_\chi} \frac{m_t}{A m_p} \left(\frac{\mu_r}{\mu_p} \right)^2 \sqrt{\langle v^2 \rangle} \frac{1}{Q_0(A)} A^2 \sigma_N^{\text{coh}} \left(\frac{dt}{du} \right) \Big|_{\text{coh}} \quad (4)$$

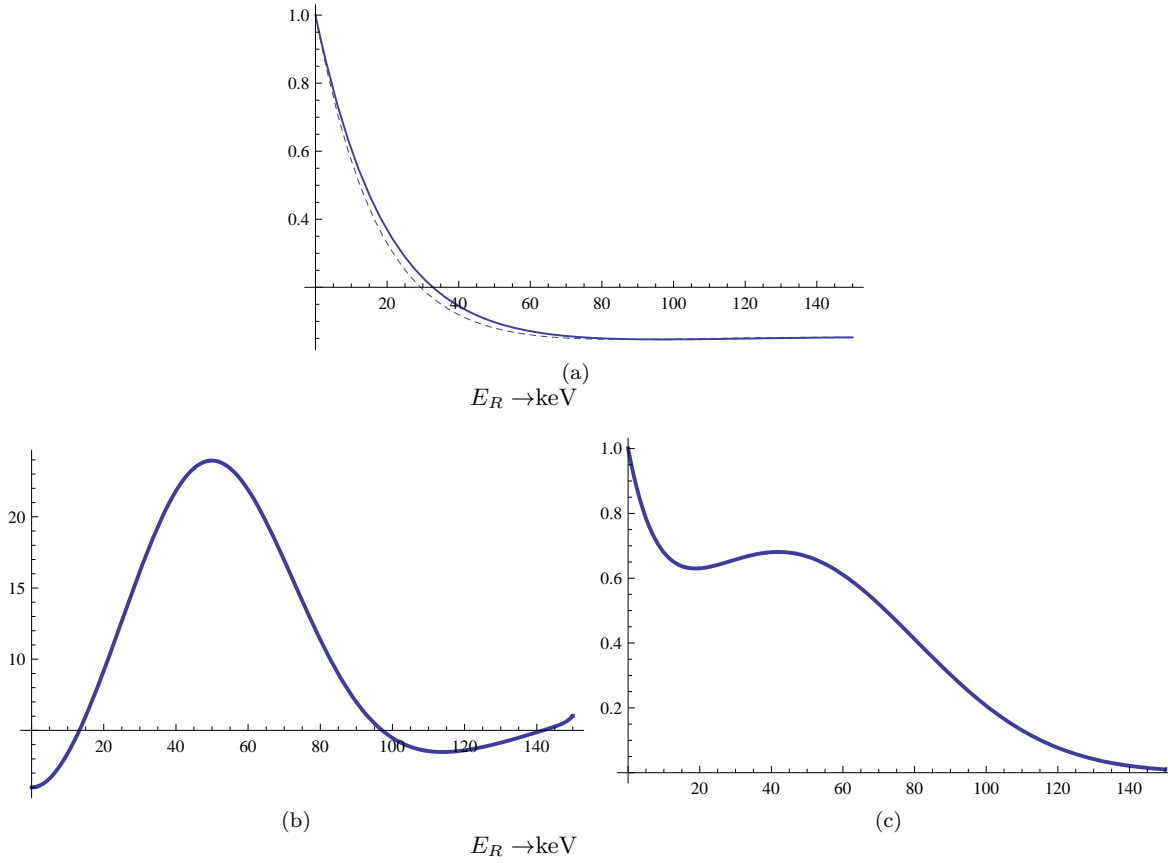


Figure 1: (a) The spin structure function, solid line, and the square of the form factor for ^{127}I as a function of the energy transfer in keV involving the ground state of ^{127}I , and the spin structure function related to the excited state of (b) of ^{127}I and (c) as in (b) for the ^{129}Xe target.

with μ_r (μ_p) the WIMP-nucleus (nucleon) reduced mass and A is the nuclear mass number. m_χ is the WIMP mass, $\rho(\chi)$ is the WIMP density in our vicinity, assumed to be 0.3 GeV cm^{-3} , and m_t the mass of the target.

Furthermore one can show that

$$\left(\frac{dt}{du} \right) \Big|_{\text{coh}} = \sqrt{\frac{2}{3}} a^2 F^2(u) \Psi_0(a\sqrt{u}), \quad \left(\frac{dh}{du} \right) \Big|_{\text{coh}} = \sqrt{\frac{2}{3}} a^2 F^2(u) \Psi_1(a\sqrt{u}) \quad (5)$$

The factor $\sqrt{2/3}$ is nothing but $v_0/\sqrt{\langle v^2 \rangle}$ since in Eq. (4) $\sqrt{\langle v^2 \rangle}$ appears. In the above expressions $a = (\sqrt{2}\mu_r b v_0)^{-1}$, v_0 the velocity of the sun around the center of the galaxy and b the nuclear harmonic oscillator size parameter characterizing the nuclear wave function. u is the energy transfer E_R in dimensionless units given by

$$u = \frac{E_R}{Q_0(A)}, \quad Q_0(A) = [m_p A b^2]^{-1} = 40 A^{-4/3} \text{ MeV} \quad (6)$$

and $F(u)$ is the nuclear form factor. Note that the parameter a depends both on the WIMP mass, the target and the velocity distribution. Note also that for a given energy transfer E_R the quantity u depends on A .

For the axial current (spin induced) contribution one finds:

$$\frac{dR_0}{dE_R} \Big|_A = \frac{\rho_\chi}{m_\chi} \frac{m_t}{A m_p} \left(\frac{\mu_r}{\mu_p} \right)^2 \sqrt{\langle v^2 \rangle} \frac{1}{Q_0(A)} \frac{1}{3} (\Omega_p - \Omega_n)^2 \sigma_N^{\text{spin}} \left(\frac{dt}{du} \right) \Big|_{\text{spin}} \quad (7)$$

with

$$\left(\frac{dt}{du}\right)\Big|_{\text{spin}} = \sqrt{\frac{2}{3}} a^2 F_{11}(u) \Psi_0(a\sqrt{u}), \quad \left(\frac{dh}{du}\right)\Big|_{\text{spin}} = \sqrt{\frac{2}{3}} a^2 F_{11}(u) \Psi_1(a\sqrt{u}), \quad (8)$$

where F_{11} is the spin response function (the square of the spin form factor). The behavior of the spin response function F_{11} for the isovector (isospin 1) channel is exhibited in Fig. 1. The other spin response functions F_{01} and F_{00} are, in our normalization, almost identical to the one shown. Note that, in the cases shown in Fig. 1, the spin response functions are not different from the square of the form factors entering the coherent mode. Thus, except for the scale of the event rates, the behavior of the coherent and the spin modes is almost identical.

Integrating the above differential rates we obtain the total rate including the time averaged rate and the relative modulation amplitude h for each mode given by:

$$R_{\text{coh}} = \frac{\rho_\chi}{m_\chi} \frac{m_t}{Am_p} \left(\frac{\mu_r}{\mu_p}\right)^2 \sqrt{\langle v^2 \rangle} A^2 \sigma_N^{\text{coh}} t_{\text{coh}}, \quad t_{\text{coh}} = \int_{E_{th}/Q_0(A)}^{(y_{\text{esc}}/a)^2} \frac{dt}{du}\Big|_{\text{coh}} du \quad (9)$$

$$R_{\text{spin}} = \frac{\rho_\chi}{m_\chi} \frac{m_t}{Am_p} \left(\frac{\mu_r}{\mu_p}\right)^2 \sqrt{\langle v^2 \rangle} \frac{1}{3} (\Omega_p - \Omega_n)^2 \sigma_N^{\text{spin}} t_{\text{spin}} \quad t_{\text{spin}} = \int_{E_{th}/Q_0(A)}^{(y_{\text{esc}}/a)^2} \frac{dt}{du}\Big|_{\text{spin}} du \quad (10)$$

for each mode (spin and coherent). $E_{th}(A)$ is the energy threshold imposed by the detector.

Using the expressions for nucleon cross sections, (9) and (10), we can obtain the total rates. These expressions contain the following parts: i) the parameter t , which contain the effect of the velocity distribution and the nuclear form factors ii) the elementary nucleon cross sections iii) the nuclear physics input (nuclear spin spin ME as mentioned above.

IV. SOME RESULTS

For purposes of illustration we will employ the nucleon cross sections obtained in a recent work [46], without committing ourselves to that particular model. From expressions (9) and (10), we can obtain the total rates. These expressions contain the following parts: i) the parameter t , which contain the effect of the velocity distribution and the nuclear form factors ii) the elementary nucleon cross sections iii) the nuclear physics input (nuclear spin spin ME)

We have seen that in the model we are going to employ [46] for demonstrating purposes, there is no A^2 or Z^2 coherence and the isovector spin induced cross section is the only possibility.

A. The differential event rates

The differential event rates, perhaps the most interesting from an experimental point of view, depend on the WIMP mass. So we can only present them for some select masses. Considerations based on the relic abundance of the WIMP in this model lead to the conclusion that it has a mass between 80 and 200 GeV. This the WIMP mass range of interest to us. For illustration purposes, however, we have decided to present some results also for lighter WIMPs. Our results for the differential rates are exhibited in Fig. 2.

B. The total event rates

We are interested here in the spin induced rates become relevant. Such results for the time averaged total rate are shown in Figs 3. The obtained results in the case of ^{129}Xe are a bit different due to the somewhat different static spin ME.

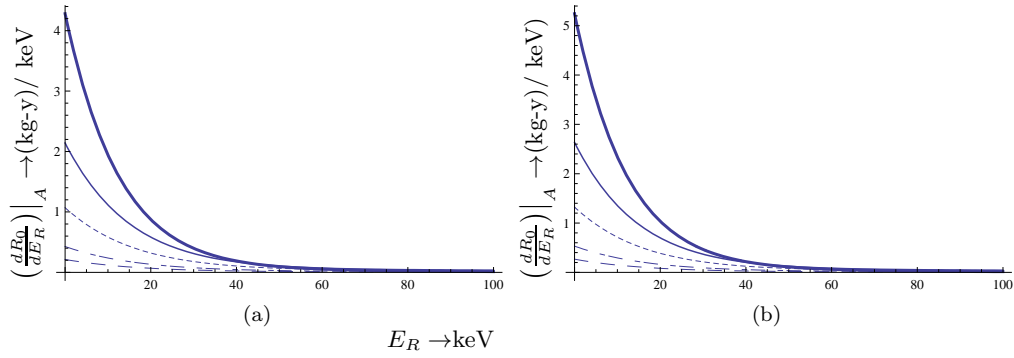


Figure 2: We show the time average differential rate $\left. \frac{dR_0}{dE_R} \right|_A$, as a function of the recoil energy E_R in keV for elastic scattering. These results correspond to the spin mode in the case of ^{127}I (a) and ^{129}Xe (b). The graphs from top to bottom correspond to WIMP masses (50, 100, 200, 500, 1000) GeV. The escape velocity was taken to be $v_{esc} = 2.8v_0$. The effect of quenching has not been included.

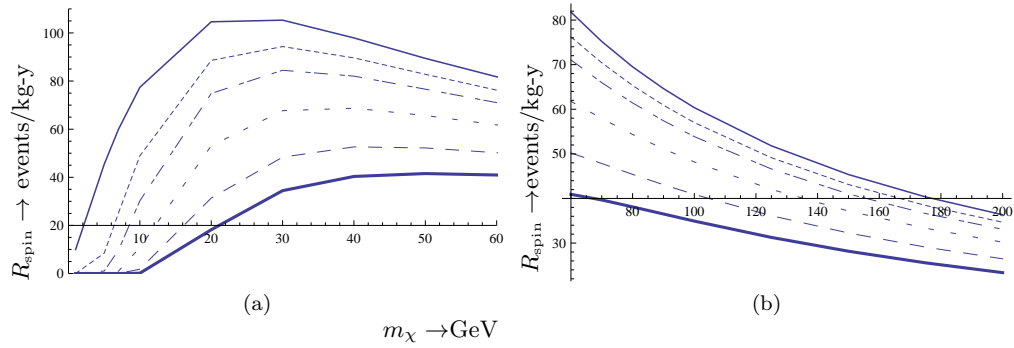


Figure 3: The predicted time averaged total rate R_{spin} for ^{127}I restricted to the small WIMP mass regime (a) and its restriction to the WIMP mass range relevant to our model (b). The highest curve corresponds to zero threshold and the lowest to a threshold of 10 keV. The effect of quenching has not been included.

V. TRANSITIONS TO EXCITED STATES

Transitions to excited states are normally forbidden, except in some odd nuclei that have low lying excited states. Then transitions to excited states are possible due to the spin. They most favorable are expected to be those that based on the total angular momentum of the states involved appear to be Gamow-Teller like transitions. A good possibility is the $7/2^+$ state of ^{127}I , which is at 57.6 keV above the $5/2^+$ ground state, and the $3/2^+$ state of ^{129}Xe at 39.6 keV. Inelastic transitions look like a Gamow-Teller like, $\Delta J = 1$, but, unfortunately, the dominant component of the wave function is not $\Delta \ell = 0$. So the spin ME entering the inelastic component may be suppressed.

A. Elementary considerations

The first criterion is to have a large elementary nucleon cross section. On general grounds, which have to do with the transition from the quark level, where particle calculations are involved to the nucleon level, only the isovector amplitude is important. There exist particle models that predict

such large cross sections. Since, however, the accessible excited states involve targets with large A , the branching ratio to the excited state is going to be significant only if the coherent nucleon cross section happens to be small. There exist particle models that satisfy this criterion. The WIMP spin 3/2 model discussed above [46] satisfies this criterion. In fact this WIMP is expected to be a Majorana Fermion, in which case the (neutron) coherent event rate vanishes. Another possibility is in supersymmetry in the co-annihilation region [47], where the ratio of the spin to coherent nucleon cross section, depending on $\tan\beta$ and the WIMP mass, which is in the range 200-500 GeV, can be as large as 10^3 . In a region of the model space the ratio of the elastic spin cross section to the coherent can be as large as 10%. More recent calculations in the supersymmetric $SO(10)$ model [48], also in the co-annihilation region, predict large spin to coherent cross section ratio, of the order of 2×10^3 and a WIMP mass of about 850 GeV. Thus from the particle physics point of view the prospect of getting an appreciable branching ratio is not discouraging.

B. Isotope considerations

Transitions to excited states are normally forbidden, except in some odd nuclei that have low lying excited states with $E \leq 100$ keV, because WIMP energy is mostly below 150 KeV. Then transitions to excited states are possible due to the spin interaction with SD WIMPs.

Possible odd nuclei involved in DM detectors used for WIMP searches are the 57.6 keV state in ^{127}I and the 39.6 keV state in ^{129}Xe , as given in Table I. The spin excitations of these states are not favored, because the dominant components of the relevant wave functions are characterized by $\Delta\ell \neq 0$, i.e. ℓ forbidden transitions. Nevertheless the spin transitions are possible, due to the small components as seen from the M1 γ transition rates.

Experimentally, large scale I and Xe detectors are being used at several DM collaborations with natural isotopes. The odd isotope abundance ratios are 100 % and 26% for ^{127}I and ^{129}Xe , respectively. Thus it is quite realistic to study the inelastic excitations in these nuclei to search for SD WIMPs.

In fact experimental observation of the inelastic excitation has several advantageous points. The experimental detection is discussed in section VI.

Table I: Inelastic spin excitations of ^{127}I and ^{129}Xe . A : natural abundance ratio, E : excitation energy, J_i : ground state spin parity, J_f : excited state spin parity, and $T_{1/2}$: half life.

Isotope	$A(\%)$	E (keV)	J_i	J_f	$T_{1/2}(\text{n sec})$
^{127}I	100	57.6	$5/2^+$	$7/2^+$	1.9
^{129}Xe	26.4	39.6	$1/2^+$	$3/2^+$	0.97

C. Kinematics

The evaluation of the differential rate for the inelastic transition proceeds as in the elastic discussed above except:

1. The transition spin matrix element must be used.
2. The transition spin response function must be used.
For Gamow teller like transitions, it does not vanish at zero energy transfer. So it can be normalized to one, if the static spin value is taken out of the ME.
3. The kinematics is modified.
The energy-momentum conservation reads:

$$\frac{-q^2}{2\mu_r} + v\xi q - E_x = 0, \quad E_x = \text{excitation energy} \Leftrightarrow -\frac{m_A}{\mu_r} E_R + v\xi \sqrt{2m_A E_R} + E_x = 0 \quad (11)$$

Clearly $\xi > 0$ as before. Then $\xi < 1$ and the reality of E_R impose the conditions:

$$E_R > E_0, \quad E_0 = \frac{\mu_r}{m_A} E_x, \quad v > \frac{E_x + \frac{m_A}{\mu_r} E_R}{\sqrt{2m_A E_R}} \quad (12)$$

We find it simpler to deal with the phase space in dimensionless units. Noticing that $u = (1/2)q^2 b^2$ and

$$\delta \left(\frac{-q^2}{2\mu_r} + v\xi q - E_x \right) = \delta \left(-\frac{u}{\mu_r b^2} + v\xi \frac{\sqrt{2u}}{b} - E_x \right) \Leftrightarrow \frac{b}{v\sqrt{2u}} \delta \left(\xi - \frac{E_x + u/(\mu_r b^2)}{v\sqrt{2u}} \right) \quad (13)$$

we find:

$$\int q^2 d\xi dq \delta \left(\frac{-q^2}{2\mu_r} + v\xi q - E_x \right) = \frac{1}{b^2 v} du \quad (14)$$

i.e. we recover the same expression as in the case of ground state transitions. The above constraints now read:

$$u > u_0, \quad y > a \frac{u + u_0}{\sqrt{u}} \quad (15)$$

$$u_0 = \mu_r E_x b^2, \quad a = \frac{1}{\sqrt{2}\mu_r v_0 b}, \quad u = \frac{E_R}{Q_0(A)} \quad (16)$$

It should be stressed that for transitions to excited states the energy of recoiling nucleus must be above a minimum energy, which depends on the excitation energy and the mass of the nucleus as well as the WIMP mass. This limits the inelastic scattering only for recoiling energies above the values $(E_R)_{\min}$. This explains why the rates do not increase as fast with the WIMP mass as naively expected. We should also mention that the maximum energy E_R allowed, which is limited by the maximum WIMP velocity, is more constrained in this case compared to that associated to the elastic scattering. In fact the maximum energy that can be transferred is:

$$u_{max} = \frac{1}{4} \left(\frac{y_{esc}}{a} + \sqrt{\left(\frac{y_{esc}}{a} \right)^2 - 4u_0^2} \right)^2 \quad (17)$$

The maximum energy transfers u_{max} somewhat depend on the escape velocity. For $y_{esc} = 2.8$, which corresponds to $v_{esc} = 620 \text{ km/s}$. The values u_0 , u_{max} , $(E_R)_{\min}$ and $(E_R)_{\max}$ relevant for the inelastic scattering of ^{127}I and ^{129}Xe are shown in Table II. We see that the energies $(E_R)_{\min}$ are much above threshold.

To avoid uncertainties arising from the relevant particle model, we will present the rate to the excited relative to that to the ground state (branching ratio). The differential event rate for inelastic scattering takes a form similar to the one given by Eq. 7 except that

$$\Omega_p - \Omega_n \rightarrow (\Omega_p - \Omega_n)^{\text{inelastic}}, \quad F_{11}(u) \rightarrow F_{11}(u)^{\text{inelastic}}, \quad \Psi_0(a\sqrt{u}) \rightarrow \Psi_0 \left(a \frac{u + u_0}{\sqrt{u}} \right), \quad u_0 \leq u \leq u_{max}$$

The obtained results are shown in Fig. 4

D. Branching ratios

We will evaluate the branching if the inelastic cross section to the spin induced cross section. One may renormalize it appropriately by including the coherent mode since then $\sigma_A^{\text{spin}} \rightarrow \sigma_A^{\text{spin}} + A^2 \sigma_N^{\text{coh}}$, with $\sigma_A^{\text{spin}} = (1/3)(\Omega_p - \Omega_n)^2 \sigma_N^{\text{spin}}$. As we have mention for the elastic case the form factors for

Table II: The kinematical parameters entering the inelastic scattering to the first excited state of ^{127}I and ^{129}Xe .

target	parameter	$m_\chi(\text{GeV})$				
		50	100	200	500	1000
^{127}I	u_0	0.270	0.421	0.585	0.762	0.848
	u_{max}	0.724	1.186	1.683	2.221	2.482
	$(E_R)_{\text{min}}(\text{keV})$	17.8	27.7	38.5	50.2	55.8
	$(E_R)_{\text{max}}(\text{keV})$	47.6	78.0	110.7	146.2	163.3
^{129}Xe	u_0	0.187	0.293	0.408	0.533	0.594
	u_{max}	0.762	1.227	1.732	2.283	2.551
	$(E_R)_{\text{min}}(\text{keV})$	12.1	18.9	26.3	34.0	38.3
	$(E_R)_{\text{max}}(\text{keV})$	49.0	79.1	111.6	147.2	164.4

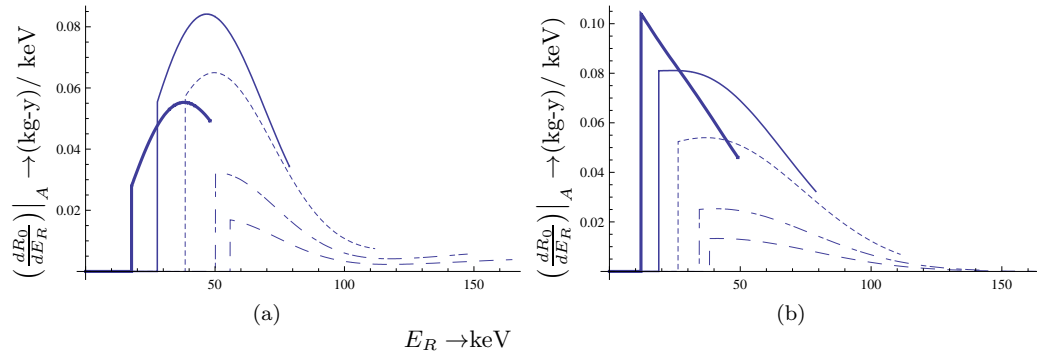


Figure 4: The same as in Fig. 2 in the case of the inelastic scattering.

the spin and the coherent mode are almost the same, which means that the shape of the differential rates are similar. We will restrict ourselves in the isovector transition. This is the case in the spin 3/2 particle model and, in general, it is expected to be dominant [49] due to considerations related to the spin of the nucleon. In the case of ^{127}I the spin ME to the excited state divided by that involving the ground state is 0.076 [44]. The spin response function (see Fig. 1), in the region of interest to us favors the excited state, which compensates for the smallness of the static spin value. In the case of ^{129}Xe this ratio 0.326 but the spin structure function is not so favorable, see Fig. 1. Our results for the differential rate are shown in Fig. 5. The individual differential rates, are, of course, suppressed at high energy transfer due to the nuclear form factor, which pretty much cancels in the ratio.

Under the same assumptions the branching ratio, i.e. the ratio of the total rates, is sketched in fig. 6.

Since the elastic event rate is reduced by the threshold effects, but the inelastic transition is not affected by such effects, we expect the branching ratio to be increasing as the threshold energy is increasing. The situation is exhibited in Fig. 7.

VI. EXPERIMENTAL ASPECTS OF INELASTIC NUCLEAR EXCITATIONS

In this section, we discuss experimental aspects of SD WIMP studies by measuring inelastic nuclear excitations. So far SD and SID WIMPs have been studied experimentally by measuring nuclear recoils of elastic scatterings.

SD WIMPs may show fairly appreciable cross sections of inelastic spin excitations, as shown in

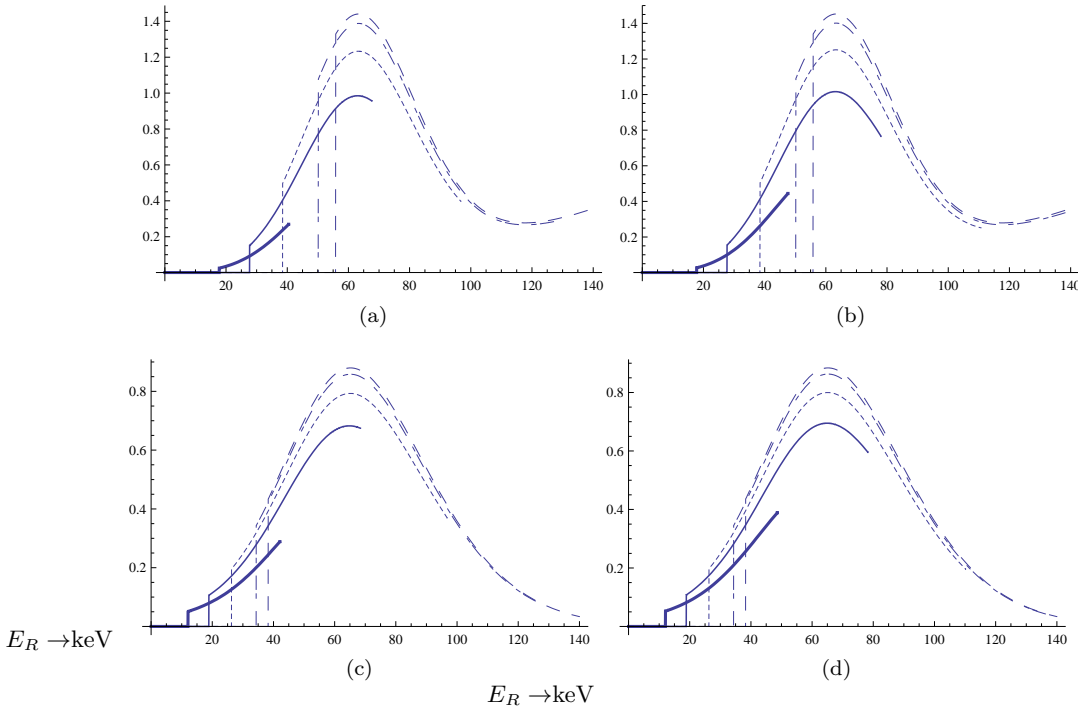


Figure 5: The ratio of the differential rates, $\frac{dR(\text{excited})}{dE_R} / \frac{dR(\text{gs})}{dE_R}$, as a function of the recoil energy E_R in keV. The thick solid, solid, dotted, dashed-dotted and dashed curves correspond to WIMP masses 50, 100, 200, 500 and 1000 GeV. In panel (a) we show the results for $y_{esc} = 2.5$ and in (b) for rate $y_{esc} = 2.8$. In (c) and (d) the same as in (a) and (b) for ^{129}Xe . Only the spin mode has been taken into account. The effect of quenching has not been included. The dependence on the escape velocity in the range of the accepted values is mild.

previous sections. Experimentally, inelastic nuclear excitations provide unique opportunities for studying SD WIMPs. Inelastic excitations are studied by two ways, A: singles measurement of both the nuclear recoil energy E_R and the decaying γ -ray energy E_γ in one detector, and B: coincidence measurement of the nuclear recoil and the γ -ray in two separate detectors. The merits of each of them are as follows.

A: Singles measurement

The large energy signal is obtained by summing the nuclear recoil signal and the γ ray signal. It is given as

$$E(ex) = E_\gamma + Q(E_R(ex))E_R(ex), \quad (18)$$

where $E_R(ex)$ is the nuclear recoil energy, E_γ is the excitation energy and $Q(E_R(ex))$ is the quenching factor for the recoil energy signal. In most scintillation and ionization detectors, the quenching factor is as small as $Q(E_R(ex)) \approx 0.1 - 0.05$. Therefore the energy deposit is mainly the excitation energy. This is much larger than just the recoil energy signal of $E(gr) = Q(E_R(gr))$, which is much quenched, depending on the detectors.

The sharp rise of the energy spectrum at the energy of $E_\gamma + Q(E_{min})E_{min}$, where E_{min} is the minimum energy transfer to the recoil nucleus. This makes it possible to identify the WIMP nuclear interaction. On the other hand, the recoil energy spectrum $E_R(gr)$ is continuum like back ground at the low energy region, and thus is hard to be identified.

$E(ex)$ is well above the detector threshold $E(th)$, while the main part of $E(gr)$ is cutoff by $E(th)$. Accordingly, the event rate $R(ex)$ is about the same order of magnitude as $R(gr)$ for SD WIMPs

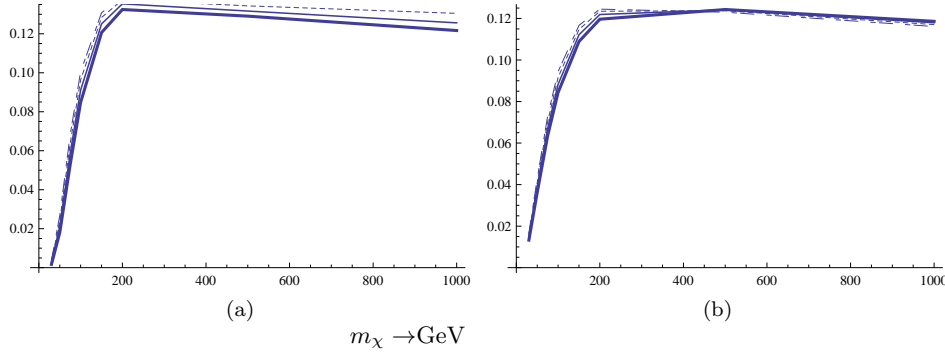


Figure 6: A sketch of the ratio of the total rates, $R(\text{excited})/R(\text{gs})$, as a function of the WIMP mass in GeV for ^{127}I (a) and ^{129}Xe (b). The dependence on the escape velocity is not visible. Only the spin mode has been taken into account. The effect of quenching has not been included.

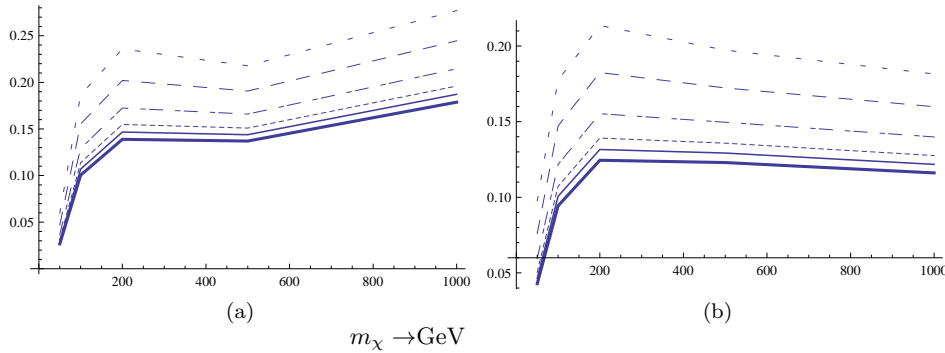


Figure 7: A sketch of the ratio of the total rates, $R(\text{excited})/R(\text{gs})$, as a function of the WIMP mass in GeV for $y=2.8$ in the case ^{127}I (a) and ^{129}Xe (b) by varying the energy threshold. From bottom up the threshold values are 0, 1, 2, 3, 4, 7 and 10 keV. Only the spin mode has been taken into account. The effect of quenching has not been included.

although the inelastic cross section is much smaller than the elastic one.

B: coincidence measurement

The nuclear recoil signal and the γ ray signal from adjacent two detector layers among a multi-layer detector array are measured in coincidence. Here WIMP hits one layer and the γ ray escapes from the layer and deposits the energy at the adjacent layer. The coincidence measurement reduces greatly BG counts. The γ ray energy signal is not quenched and is as large as 30-60 keV. It shows a sharp peak to be identified easily.

The one layer of the detector has to be as thin as sub mm to make it possible for the γ ray to escape from the layer. The detection efficiency is an order of 0.1 - 0.3, depending very much on the γ ray escape probability.

The typical energy spectra to be measured experimentally for the elastic and inelastic transitions of ^{127}I and ^{129}Xe are shown in Figs 8 and 9. Here we assumed detectors with the quenching factor of $Q=0.05$ and the energy threshold of $E(th) = 1.6$ keV. The yield in y axis is the one per unit energy of the electron equivalent energy, i.e. QE_R and the energy in x axis is the electron equivalent one.

We note that the yield is enlarged by a factor $1/Q=20$, while the energy is shrunk by a factor $Q=0.05$. The low energy part of the elastic scattering is cut off by the threshold energy of 1.6 keV electron equivalent energy, i.e. 32 keV recoil energy.

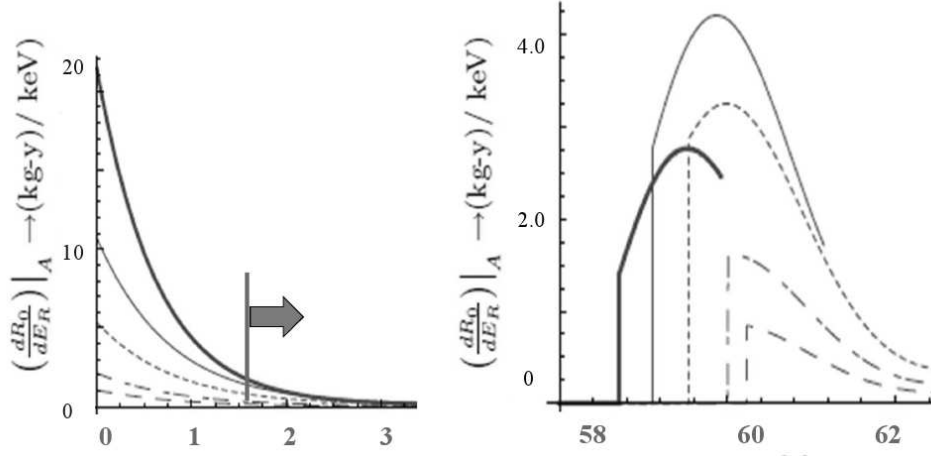


Figure 8: Energy spectrum for WIMP ^{127}I elastic scattering (left-hand side) and that for the 57.6 keV excited state inelastic scattering (right hand side). Quenching factor is $Q=0.05$, and the energy threshold is $E(th) = 1.6$ keV. The x and y scales are the electron-equivalent energy and the rate per unit electron equivalent energy.

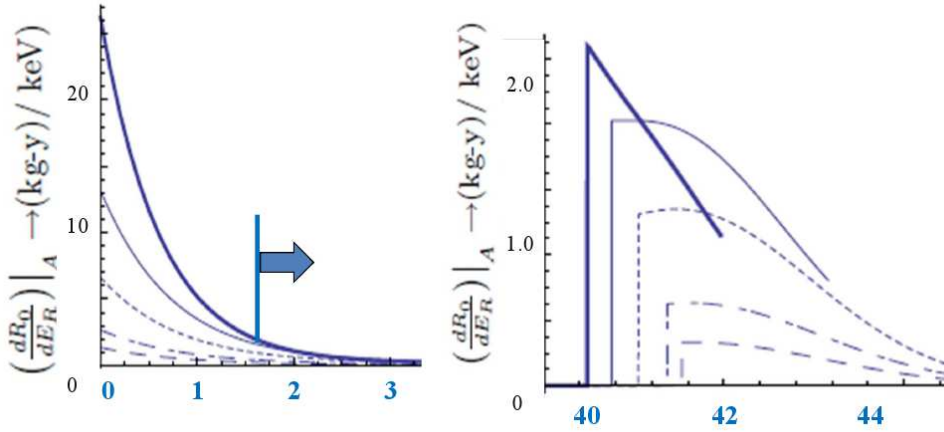


Figure 9: Energy spectrum for WIMP ^{129}Xe elastic scattering (left-hand side) and that for the 39.6 keV excited state inelastic scattering (right hand scale). Otherwise the notation is the same as in 8.

VII. CONCLUDING REMARKS

SI and SD WIMPs have extensively been studied, so far, by measuring elastic nuclear recoils. The elastic scattering of SI WIMPs is coherent scattering, thus the cross section is enhanced by the factor A^2 with A being the nuclear mass number. On the other hand the elastic cross section of SD WIMPs is, in general, smaller by 2-3 orders of magnitude than that for SI WIMPs because of lack of coherence. It may, however, compete with the coherent in models in which the spin induced nucleon cross section is much larger than the one due to a scalar interaction. We have seen that there exist viable such particle models. In such cases the inelastic WIMP-nucleus scattering becomes important.

Indeed the inelastic scattering via spin interaction provides a new opportunity for studying SD

WIMPs. Experimentally, observation of both the nuclear recoils and the γ ray following the excited state does lead to the large energy signal of the unquenched E_γ and the sharp rise of the energy spectrum at around E_γ . Even though the SD inelastic cross section is smaller than the SD elastic one, the inelastic event rate is comparable with the elastic one, since the inelastic signal is well beyond the detector threshold energy, while the elastic signal is mostly cut off by the detector threshold.

In short, the present paper shows that the inelastic scattering opens a new powerful way to search for SD WIMPs.

In the present paper we discussed mainly the inelastic excitations of ^{127}I and ^{129}Xe by using the I and Xe detectors. Another possible isotope is the ^{73}Ge in high energy resolution Ge detectors. We are currently evaluating the relevant nuclear matrix elements [50] (static spin and structure functions) and we will discuss this interesting case in a forthcoming article.

-
- [1] S. Hanany *et al.* *Astrophys. J.* **545**, L5 (2000);
J.H.P. Wu *et al.* *Phys. Rev. Lett.* **87**, 251303 (2001);
M.G. Santos *et al.* *Phys. Rev. Lett.* **88**, 241302 (2002).
 - [2] P. D. Mauskopf *et al.* *Astrophys. J.* **536**, L59 (2002);
S. Mosi *et al.* *Prog. Nuc.Part. Phys.* **48**, 243 (2002);
S. B. Ruhl *et al.*, astro-ph/0212229 and references therein.
 - [3] N. W. Halverson *et al.* *Astrophys. J.* **568**, 38 (2002)
L. S. Sievers *et al.*: astro-ph/0205287 and references therein.
 - [4] G. F. Smoot and *et al.* (COBE Collaboration), *Astrophys. J.* **396**, L1 (1992).
 - [5] A. H. Jaffe and *et al.*, *Phys. Rev. Lett.* **86**, 3475 (2001).
 - [6] D. N. Spergel and *et al.*, *Astrophys. J. Suppl.* **148**, 175 (2003).
 - [7] D. Spergel *et al.*, *Astrophys. J. Suppl.* **170**, 377 (2007), [arXiv:astro-ph/0603449v2].
 - [8] The Planck Collaboration, A.P.R. Ade *et al.*, arXiv:1303.5076 [astro-ph.CO].
 - [9] D. P. Bennett and *et al.*, *Phys. Rev. Lett.* **74**, 2867 (1995).
 - [10] P. Ullio and M. Kamiokowski, *JHEP* **0103**, 049 (2001).
 - [11] A. Bottino and *et al.*, *Phys. Lett. B* **402**, 113 (1997).
 - [12] R. Arnowitt and P. Nath, *Phys. Rev. Lett.* **74**, 4592 (1995).
 - [13] R. Arnowitt and P. Nath, *Phys. Rev. D* **54**, 2374 (1996), hep-ph/9902237.
 - [14] A. Bottino *et al.*, *Phys. Lett. B* **402**, 113 (1997).
R. Arnowitt. and P. Nath, *Phys. Rev. Lett.* **74**, 4592 (1995); *Phys. Rev. D* **54**, 2374 (1996);
hep-ph/9902237;
V. A. Bednyakov, H.V. Klapdor-Kleingrothaus and S.G. Kovalenko, *Phys. Lett. B* **329**, 5 (1994).
 - [15] J. Ellis and L. Roszkowski, *Phys. Lett. B* **283**, 252 (1992).
 - [16] M. E. Gómez and J. D. Vergados, *Phys. Lett. B* **512**, 252 (2001); hep-ph/0012020.
M. E. Gómez, G. Lazarides and Pallis, C., *Phys. Rev.D* **61**, 123512 (2000) and *Phys. Lett. B* **487**, 313 (2000).
 - [17] J. Ellis, and R. A. Flores, *Phys. Lett. B* **263**, 259 (1991); *Phys. Lett. B* **300**, 175 (1993); *Nucl. Phys. B* **400**, 25 (1993).
 - [18] S. Nussinov, *Phys. Lett. B* **279**, 111 (1992).
 - [19] S. B. Gudnason, C. Kouvaris, and F. Sannino, *Phys. Rev. D* **74**, 095008 (2006), arXiv:hep-ph/0608055.
 - [20] R. Foot, H. Lew, and R. R. Volkas, *Phys. Lett. B* **272**, 676 (1991).
 - [21] R. Foot, *Phys. Lett. B* **703**, 7 (2011), [arXiv:1106.2688].
 - [22] G. Servant and T. M. P. Tait, *Nuc. Phys. B* **650**, 391 (2003).
 - [23] V. Oikonomou, J. Vergados, and C. C. Moustakidis, *Nuc. Phys. B* **773**, 19 (2007).
 - [24] J. D. Vergados, *Lect. Notes Phys.* **720**, 69 (2007), hep-ph/0601064.
 - [25] A. Djouadi and M. K. Drees, *Phys. Lett. B* **484**, 183 (2000); S. Dawson, *Nucl. Phys. B* **359**, 283 (1991);
M. Spira *et al.*, *Nucl. Phys. B* **453**, 17 (1995).
 - [26] M. Drees and M. M. Nojiri, *Phys. Rev. D* **48**, 3843 (1993); *Phys. Rev. D* **47**, 4226 (1993).
 - [27] T. P. Cheng, *Phys. Rev. D* **38**, 2869 (1988); H-Y. Cheng, *Phys. Lett. B* **219**, 347 (1989).
 - [28] M. T. Ressell *et al.*, *Phys. Rev. D* **48**, 5519 (1993); M.T. Ressell and D. J. Dean, *Phys. Rev. C* **56**, 535 (1997).
 - [29] P. C. Divari, T. S. Kosmas, J. D. Vergados, and L. D. Skouras, *Phys. Rev. C* **61**, 054612 (2000).
 - [30] J. D. Vergados, *Phys. Rev. D* **67**, 103003 (2003), hep-ph/0303231.
 - [31] J. Vergados, *J. Phys. G* **30**, 1127 (2004), [arXiv:hep-ph/0406134].
 - [32] J. Vergados and A. Faessler, *Phys. Rev. D* **75**, 055007 (2007).

- [33] U. Chattopadhyay, A. Corsetti, and P. Nath, Phys. Rev. D **68**, 035005 (2003).
- [34] U. Chattopadhyay and D. Roy, Phys. Rev. D **68**, 033010 (2003), hep-ph/0304108.
- [35] B. Murakami and J. Wells, Phys. Rev. D p. 015001 (2001), hep-ph/0011082.
- [36] M. W. Goodman and E. Witten, Phys. Rev. D **31**, 3059 (1985).
- [37] H. Ejiri, K. Fushimi, and H. Ohsumi, Phys. Lett. B **317**, 14 (1993).
- [38] J. Engel, S. Pittel, and P. Vogel, Phys. Rev. C **50**, 1702 (1994).
- [39] P. Vogel and J. Engel, Phys. Rev. **D 39**, 3378 (1989).
- [40] F. I. L. Krauss and G. Maino, Phys. Lett B **250**, 220 (1991).
- [41] M. Nikolaev and H. Klapdor-Kleingrothaus, Z. Phys. A **345**, 373 (1975).
- [42] E. Homlund and M. Kortelainen and T. S. Kosmas and J. Suhonen and J. Toivanen, Phys. Lett B, **584**,31 (2004); Phys. Atom. Nucl. **67**, 1198 (2004).
- [43] J. D. Vergados, P. Quentin, and D. Strottman, IJMPE **14**, 751 (2005), hep-ph/0310365.
- [44] P. Toivanen, M. Kortelainen, J. Suhonen, and J. Toivanen, Phys. Rev. C **79**, 044302 (2009).
- [45] J. Menendez and D. Gazit and A. Schwenk, arXiv:1208.1094 (astro-ph.CO).
- [46] K. Savvidy and J. Vergados, Phys. Rev. D **87**, 075013 (2013).
- [47] M. Cannoni, Phys. Rev. D **84**, 095017 (2011).
- [48] M. Adeel Ajaib, Ilia Gogoladze, Qaisar Shafi and Cem Salih Ünlü, arXiv:1303.6964 [hep-ph].
- [49] J. Ellis and M. Karliner, CERN-TH **7072** (1993).
- [50] T. S. Kosmas *et al*, Private communication.